Comput Geosci (2007) 11:199–206
DOI 10.1007/s10596-007-9042-1

ORIGINAL PAPER

Interpretation of a two-point flux stencil for skew parallelogram grids

Ivar Aavatsmark

Received: 18 February 2005 / Accepted: 4 January 2007 / Published online: 13 February 2007

Abstract Control-volume formulations for elliptic equations often use two-point flux stencils, even for skew grids. Any two-point flux stencil may be interpreted as a multipoint flux stencil. This yields a definition of the permeability (or conductivity) tensor. Formulas for calculating the permeability tensor, based on the user-specified quantities in the two-point flux stencil, are given. Numerical test examples demonstrate the validity of the derivation.

Keywords anisotropy · control-volume discretization · error analysis · permeability tensor · two-point flux

Mathematics Subject Classifications (2000) 65N06 · 76S05 · 35R05

1 Introduction

We consider the equation

$$-\operatorname{div}(\boldsymbol{K}\operatorname{grad} p) = Q, \tag{1}$$

which is used as a model equation for the pressure in reservoir simulation. Here, $\boldsymbol{K}$ is the permeability tensor, p is the pressure, and Q is a source density. The permeability tensor is assumed to be symmetric and positive definite.

Two-point flux stencils are widely used in control-volume discretizations of Eq. (1) [4]. Such stencils approximate the flux correctly for Cartesian grids with the principal directions of the permeability tensor $\boldsymbol{K}$ aligned with the grid directions [5, 7]. For skew grids, in general, a multipoint flux approximation (MPFA) is needed [1, 3]. However, in the MPFA O-method, the flux stencil reduces to a two-point flux stencil if and only if the grid is $\boldsymbol{K}$-orthogonal. Therefore, any two-point flux stencil applied to a skew grid may be interpreted as a multipoint flux stencil. In this interpretation, the found permeability tensor $\boldsymbol{K}$ leaves the grid $\boldsymbol{K}$-orthogonal.

The opposite is not true. In general, it is impossible to use a consistent two-point flux approximation for a skew grid with a general permeability tensor.

In this paper, we show how a two-point flux stencil for a skew parallelogram grid may be interpreted as a multipoint flux stencil for a $\boldsymbol{K}$-orthogonal grid. This enables us to calculate the permeability tensor $\boldsymbol{K}$. Thus, the user-specified permeabilities on any skew parallelogram grid define the permeability tensor of the system, which is actually being simulated.

The analysis is done for two spatial dimensions only. For three spatial dimensions, it is straightforward to present the equations that determine the permeability tensor, but the equations are much more complex than in the two-dimensional case. Therefore, three-dimensional problems are not considered in this paper.

2 Interpretation of two-point flux

The flux through the edges of a parallelogram cell is determined by the geometric quantities shown in Fig. 1. Here, $\boldsymbol{\nu}_1$ is a unit vector pointing in the positive ξ-direction, and $\boldsymbol{\nu}_2$ is a unit vector pointing in the positive η-direction. Further, $\boldsymbol{n}_1$ is a unit vector normal

I. Aavatsmark (✉)
Centre for Integrated Petroleum Research,
University of Bergen, 5020 Bergen, Norway
e-mail: ivar.aavatsmark@cipr.uib.no

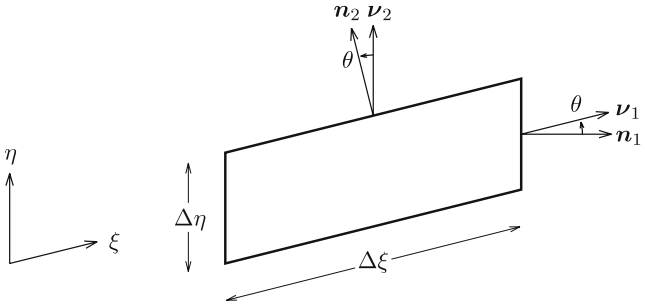

Fig. 1 Parallelogram with normal vectors $\boldsymbol{n}_1$ and $\boldsymbol{n}_2$ and tangential vectors $\boldsymbol{\nu}_1$ and $\boldsymbol{\nu}_2$

to the edge on which ξ is constant, and $\boldsymbol{n}_2$ is a unit vector normal to the edge on which η is constant. The positive direction of the vectors $\boldsymbol{n}_1$ and $\boldsymbol{n}_2$ is determined such that $\boldsymbol{n}_i \cdot \boldsymbol{\nu}_i = \cos\theta > 0$ for $i = 1, 2$, where θ is the angle between $\boldsymbol{n}_i$ and $\boldsymbol{\nu}_i$, $i = 1, 2$. If $\boldsymbol{\nu}_1$ is rotated a positive angle from $\boldsymbol{n}_1$, the angle θ is positive. The vectors $\boldsymbol{\nu}_1$ and $\boldsymbol{n}_2$ are orthogonal, and so are the vectors $\boldsymbol{n}_1$ and $\boldsymbol{\nu}_2$. The quantities $\Delta\xi$ and $\Delta\eta$ are the edge lengths in ξ-direction and η-direction, respectively.

The *Eclipse* reservoir simulator [4] uses with the `Newtran` keyword a two-point flux formula. With the above quantities, the flux through the right and the top edges of a cell is given by

$$\boldsymbol{f} = \frac{2\det[\boldsymbol{n}_1,\ \boldsymbol{n}_2]}{\Delta\xi\,\Delta\eta}\begin{bmatrix}\lambda_1(\Delta\eta)^2\Delta p_\xi\\ \lambda_2(\Delta\xi)^2\Delta p_\eta\end{bmatrix}. \tag{2}$$

Here, λ_1 and λ_2 are the user-specified permeabilities in the ξ- and the η-direction, respectively. Further, Δp_ξ and Δp_η are the pressure drops in ξ- and η-direction, measured from the cell center to the midpoint of the right and the top edge, respectively. The determinant of the matrix $[\boldsymbol{n}_1,\ \boldsymbol{n}_2]$ satisfies

$$\det[\boldsymbol{n}_1,\ \boldsymbol{n}_2] = \boldsymbol{n}_1 \cdot \boldsymbol{\nu}_1 = \boldsymbol{n}_2 \cdot \boldsymbol{\nu}_2 = \cos\theta. \tag{3}$$

In the MPFA O-method, the flux through the right and the top edges is given by [1, 3]

$$\boldsymbol{f} = \frac{2}{\Delta\xi\,\Delta\eta}\boldsymbol{D}\boldsymbol{H}\boldsymbol{D}\begin{bmatrix}\Delta p_\xi\\ \Delta p_\eta\end{bmatrix}, \tag{4}$$

where

$$\boldsymbol{H} = \frac{1}{\det[\boldsymbol{n}_1,\ \boldsymbol{n}_2]}\begin{bmatrix}\boldsymbol{n}_1^{\mathrm{T}}\boldsymbol{K}\boldsymbol{n}_1 & \boldsymbol{n}_1^{\mathrm{T}}\boldsymbol{K}\boldsymbol{n}_2\\ \boldsymbol{n}_2^{\mathrm{T}}\boldsymbol{K}\boldsymbol{n}_1 & \boldsymbol{n}_2^{\mathrm{T}}\boldsymbol{K}\boldsymbol{n}_2\end{bmatrix}, \tag{5}$$

$$\boldsymbol{D} = \mathrm{diag}(\Delta\eta,\ \Delta\xi). \tag{6}$$

Using the flux formula (4), convergence is obtained for the linear elliptic pressure Eq. (1) [3, 6]. Hence, by requiring that the flux expressions (2) and (4) are equal, the permeability tensor $\boldsymbol{K}$ may be calculated from the user-specified permeabilities λ_1 and λ_2.

Equating expressions (2) and (4) yields the equation

$$\boldsymbol{H} = \det[\boldsymbol{n}_1,\ \boldsymbol{n}_2]\ \mathrm{diag}(\lambda_1,\ \lambda_2), \tag{7}$$

i.e.,

$$\begin{aligned}\boldsymbol{n}_1^{\mathrm{T}}\boldsymbol{K}\boldsymbol{n}_1 &= (\det[\boldsymbol{n}_1,\ \boldsymbol{n}_2])^2\,\lambda_1,\\ \boldsymbol{n}_2^{\mathrm{T}}\boldsymbol{K}\boldsymbol{n}_2 &= (\det[\boldsymbol{n}_1,\ \boldsymbol{n}_2])^2\,\lambda_2,\\ \boldsymbol{n}_1^{\mathrm{T}}\boldsymbol{K}\boldsymbol{n}_2 &= 0.\end{aligned} \tag{8}$$

The last equation in system (8) is the condition for $\boldsymbol{K}$-orthogonality of the grid. Only those permeability tensors that satisfy this equation allow a consistent two-point flux approximation. Eq. (8) shows that when $\boldsymbol{K}$ is a solution of these equations, then $\lambda_i = \|\boldsymbol{K}\boldsymbol{n}_i\|_2 / \cos\theta$, $i = 1, 2$.

The system of equations (7) or (8) yields an interpretation of the quantities λ_1 and λ_2 as the cell's *apparent permeabilities*. By using the flux expression (2), the user is actually simulating on a medium with the cell permeability tensor $\boldsymbol{K}$, determined by Eqs. (7) or (8).

We now show how the permeability tensor $\boldsymbol{K}$ is determined by the apparent permeabilities λ_1 and λ_2. Let the eigenvalues of $\boldsymbol{K}$ be k_1 and k_2 with associated unit eigenvectors $\boldsymbol{e}_1$ and $\boldsymbol{e}_2$, respectively. The eigenvector $\boldsymbol{e}_1$ is rotated an angle ϕ from the vector $\boldsymbol{\nu}_1$ (see Fig. 2). Since $\boldsymbol{K}$ is symmetric, the vectors $\boldsymbol{e}_1$ and $\boldsymbol{e}_2$ are orthogonal. In the coordinate system of the eigenvectors, the permeability tensor is given by $\boldsymbol{K}_{\boldsymbol{e}_1\boldsymbol{e}_2} = \mathrm{diag}(k_1,\ k_2)$, and the edge unit normal vectors are

$$(\boldsymbol{n}_1)_{\boldsymbol{e}_1\boldsymbol{e}_2} = \begin{bmatrix}\cos(\theta+\phi)\\ -\sin(\theta+\phi)\end{bmatrix}, \qquad (\boldsymbol{n}_2)_{\boldsymbol{e}_1\boldsymbol{e}_2} = \begin{bmatrix}\sin\phi\\ \cos\phi\end{bmatrix}. \tag{9}$$

Hence, in the coordinate system of the eigenvectors, the system of equations (8) reads

$$\begin{aligned}k_1\cos^2(\theta+\phi) + k_2\sin^2(\theta+\phi) &= \lambda_1\cos^2\theta,\\ k_1\sin^2\phi + k_2\cos^2\phi &= \lambda_2\cos^2\theta,\\ k_1\cos(\theta+\phi)\sin\phi - k_2\sin(\theta+\phi)\cos\phi &= 0.\end{aligned} \tag{10}$$

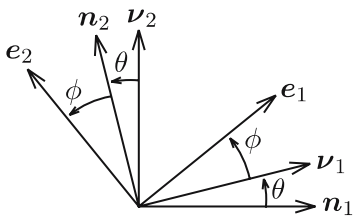

Fig. 2 Vectors $\boldsymbol{n}_i$, $\boldsymbol{\nu}_i$, and $\boldsymbol{e}_i$, $i = 1, 2$. The vector $\boldsymbol{\nu}_1$ is rotated an angle θ from $\boldsymbol{n}_1$, and the vector $\boldsymbol{e}_1$ is rotated an angle ϕ from $\boldsymbol{\nu}_1$

To solve the system of equations (10), it is suitable to introduce the following new quantities: the *anisotropy ratio*

$$\kappa = \frac{k_1}{k_2}, \tag{11}$$

the *apparent anisotropy ratio*

$$\mu = \frac{\lambda_1}{\lambda_2}, \tag{12}$$

and the ratio between the mean permeability and the mean apparent permeability

$$\rho = \left(\frac{k_1 k_2}{\lambda_1 \lambda_2}\right)^{1/2}. \tag{13}$$

With these quantities, the system of equations (10) may be written as

$$\rho\left(\kappa^{1/2}\cos^2(\theta+\phi)+\kappa^{-1/2}\sin^2(\theta+\phi)\right)=\mu^{1/2}\cos^2\theta, \tag{14}$$

$$\rho\left(\kappa^{1/2}\sin^2\phi+\kappa^{-1/2}\cos^2\phi\right)=\mu^{-1/2}\cos^2\theta, \tag{15}$$

$$\kappa^{1/2}\cos(\theta+\phi)\sin\phi-\kappa^{-1/2}\sin(\theta+\phi)\cos\phi=0. \tag{16}$$

The system of equations (14), (15), and (16) is solved as follows. From Eq. (16), the anisotropy ratio κ may be expressed as

$$\kappa = \frac{\sin(\theta+\phi)\cos\phi}{\cos(\theta+\phi)\sin\phi}. \tag{17}$$

Dividing Eq. (14) by Eq. (15) yields

$$\frac{\kappa\cos^2(\theta+\phi)+\sin^2(\theta+\phi)}{\kappa\sin^2\phi+\cos^2\phi}=\mu. \tag{18}$$

Substituting expression (17) into Eq. (18) gives

$$\begin{aligned}\mu &= \frac{\frac{\sin(\theta+\phi)\cos\phi}{\cos(\theta+\phi)\sin\phi}\cos^2(\theta+\phi)+\sin^2(\theta+\phi)}{\frac{\sin(\theta+\phi)\cos\phi}{\cos(\theta+\phi)\sin\phi}\sin^2\phi+\cos^2\phi}\\ &= \frac{\sin(\theta+\phi)\cos^2(\theta+\phi)\cos\phi+\sin^2(\theta+\phi)\cos(\theta+\phi)\sin\phi}{\sin(\theta+\phi)\sin^2\phi\cos\phi+\cos(\theta+\phi)\sin\phi\cos^2\phi}\\ &= \frac{\sin(\theta+\phi)\cos(\theta+\phi)}{\sin\phi\cos\phi}\\ &= \frac{\sin 2(\theta+\phi)}{\sin 2\phi}.\end{aligned} \tag{19}$$

Hence,

$$\sin 2\theta\cos 2\phi+\cos 2\theta\sin 2\phi=\mu\sin 2\phi, \tag{20}$$

i.e.,

$$\tan 2\phi = \frac{\sin 2\theta}{\mu-\cos 2\theta}. \tag{21}$$

Finally, the ratio ρ is determined from Eq. (15),

$$\rho = \frac{\cos^2\theta}{\kappa\sin^2\phi+\cos^2\phi}\left(\frac{\kappa}{\mu}\right)^{1/2}. \tag{22}$$

Using expression (17) for κ and expression (19) for μ, one finds

$$\begin{aligned}\rho &= \frac{\cos^2\theta}{\frac{\sin(\theta+\phi)\cos\phi}{\cos(\theta+\phi)\sin\phi}\sin^2\phi+\cos^2\phi}\left(\frac{\frac{\sin(\theta+\phi)\cos\phi}{\cos(\theta+\phi)\sin\phi}}{\frac{\sin(\theta+\phi)\cos(\theta+\phi)}{\sin\phi\cos\phi}}\right)^{1/2}\\ &= \frac{\cos(\theta+\phi)\cos^2\theta}{\sin(\theta+\phi)\sin\phi\cos\phi+\cos(\theta+\phi)\cos^2\phi}\left(\frac{\cos^2\phi}{\cos^2(\theta+\phi)}\right)^{1/2}\\ &= \frac{\cos^2\theta}{\sin(\theta+\phi)\sin\phi+\cos(\theta+\phi)\cos\phi}\\ &= \cos\theta.\end{aligned} \tag{23}$$

Expressions (17), (21), and (23) contain the solution of the system of equations (14), (15), and (16). The solution reads

$$\boxed{\begin{aligned}\phi &= \frac{1}{2}\arctan\frac{\sin 2\theta}{\mu-\cos 2\theta},\\ \kappa &= \frac{\tan(\theta+\phi)}{\tan\phi},\\ \rho &= \cos\theta.\end{aligned}} \tag{24}$$

Here, $|\theta|<\pi/2$ and $\mu>0$. The solution satisfies $|\phi|<\pi/4$ and $\kappa>0$. Further, the solution obeys the symmetry relations $\phi(-\theta,\mu)=-\phi(\theta,\mu)$ and $\kappa(-\theta,\mu)=\kappa(\theta,\mu)$.

Having found solution (24), we may also express the permeability tensor $\boldsymbol{K}$ in coordinates aligned with the grid. In the coordinate system of the eigenvectors $\boldsymbol{e}_1$ and $\boldsymbol{e}_2$, the tensor reads

$$\boldsymbol{K}_{\boldsymbol{e}_1\boldsymbol{e}_2} = \rho(\lambda_1\lambda_2)^{1/2}\,\mathrm{diag}\left(\kappa^{1/2},\kappa^{-1/2}\right). \tag{25}$$

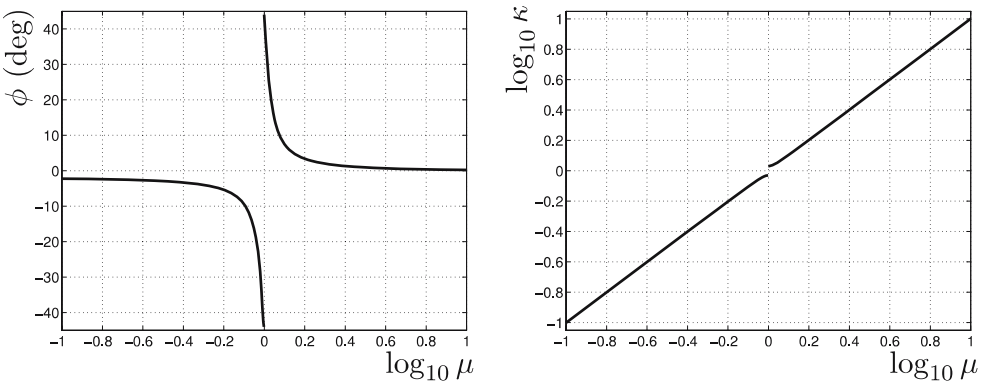

Fig. 3 Solution (24) for $\theta = 2°$. Left: $\phi(\theta, \mu)$. Right: $\kappa(\theta, \mu)$

In the coordinate system of the orthogonal vectors $\boldsymbol{v}_1$ and $\boldsymbol{n}_2$, the tensor is given by

$$\boldsymbol{K}_{\boldsymbol{v}_1\boldsymbol{n}_2} = \boldsymbol{R}(-\phi)\boldsymbol{K}_{\boldsymbol{e}_1\boldsymbol{e}_2}\boldsymbol{R}(\phi), \tag{26}$$

where

$$\boldsymbol{R}(\phi) = \begin{bmatrix} \cos\phi & \sin\phi \\ -\sin\phi & \cos\phi \end{bmatrix}. \tag{27}$$

Hence,

$$\boldsymbol{K}_{\boldsymbol{v}_1\boldsymbol{n}_2} = \rho(\lambda_1\lambda_2)^{1/2} \times \begin{bmatrix} \kappa^{1/2}\cos^2\phi + \kappa^{-1/2}\sin^2\phi & \left(\kappa^{1/2} - \kappa^{-1/2}\right)\cos\phi\sin\phi \\ \left(\kappa^{1/2} - \kappa^{-1/2}\right)\cos\phi\sin\phi & \kappa^{1/2}\sin^2\phi + \kappa^{-1/2}\cos^2\phi \end{bmatrix}. \tag{28}$$

Similarly, in the coordinate system of the orthogonal vectors $\boldsymbol{n}_1$ and $\boldsymbol{v}_2$, the tensor reads $\boldsymbol{K}_{\boldsymbol{n}_1\boldsymbol{v}_2} = \boldsymbol{R}(-(\theta + \phi))\boldsymbol{K}_{\boldsymbol{e}_1\boldsymbol{e}_2}\boldsymbol{R}(\theta + \phi)$, i.e., $\boldsymbol{K}_{\boldsymbol{n}_1\boldsymbol{v}_2}$ is obtained from Eq. (28), by replacing ϕ with $\theta + \phi$.

3 Discussion of the solution

The solutions $\phi(\theta, \mu)$ and $\kappa(\theta, \mu)$ in Eq. (24) may be displayed for fixed θ with varying μ or for fixed μ with varying θ. Below, the former form is chosen.

For any fixed θ satisfying $|\theta| < \pi/4$, the expression for $\phi(\theta, \mu)$ in Eq. (24) has a singularity at some positive μ. The singularity appears at $\mu = \mu_0$, where

$$\mu_0 = \cos 2\theta, \qquad |\theta| < \pi/4. \tag{29}$$

The limiting values of $\phi(\theta, \mu)$ for θ fixed and $\mu = \mu_0$ are

$$\begin{aligned} \phi(\theta, \mu_0+) &= \operatorname{sgn}\theta \cdot \pi/4, \\ \phi(\theta, \mu_0-) &= -\operatorname{sgn}\theta \cdot \pi/4. \end{aligned} \tag{30}$$

This singularity also appears for $\kappa(\theta, \mu)$ with limiting values

$$\begin{aligned} \kappa(\theta, \mu_0+) &= \tan(|\theta| + \pi/4), \\ \kappa(\theta, \mu_0-) &= 1/\tan(|\theta| + \pi/4). \end{aligned} \tag{31}$$

The values of κ at each side of μ_0 are the reciprocals of each other, and the values of ϕ at each side of μ_0 differ by $\pi/2$. Hence, at the singularity, the eigenvectors simply exchange indices. Therefore, μ_0 is a singular point for the functions ϕ and κ, but not for the permeability tensor $\boldsymbol{K}$.

Figures 3, 4, 5, and 6 show the solutions $\phi(\theta, \mu)$ and $\kappa(\theta, \mu)$ for the following grid skewness angles θ: 2, 5, 15, and 40°. The singularity at $\mu_0 = \cos 2\theta$ is clearly shown.

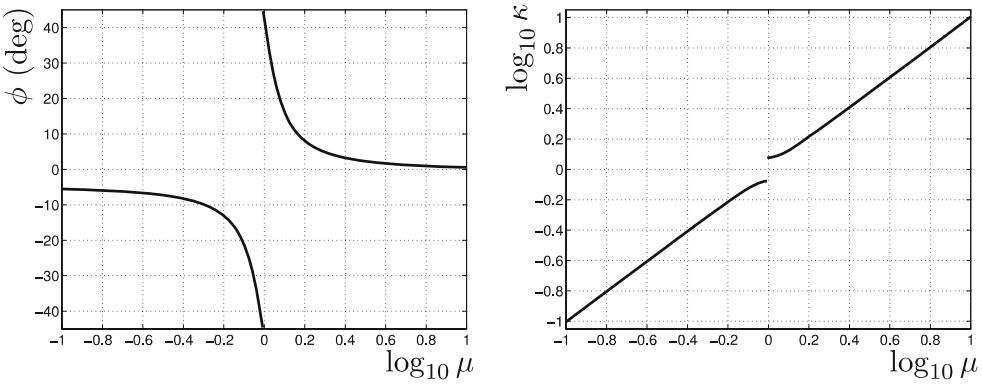

Fig. 4 Solution (24) for $\theta = 5°$. Left: $\phi(\theta, \mu)$. Right: $\kappa(\theta, \mu)$

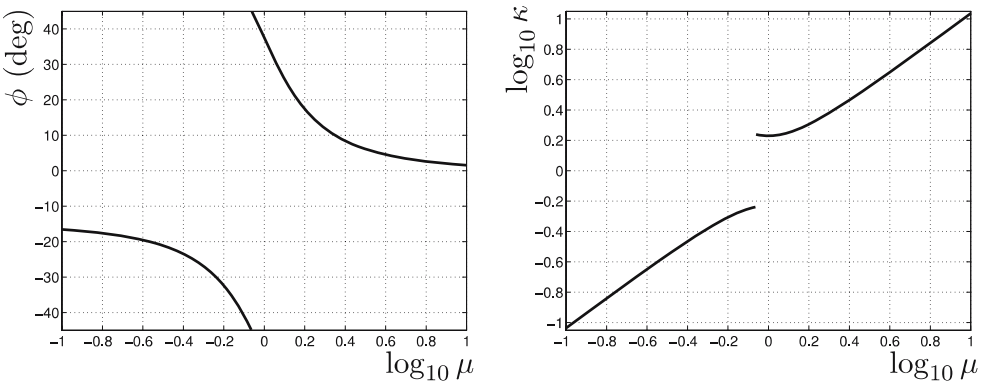

Fig. 5 Solution (24) for $\theta = 15°$. Left: $\phi(\theta, \mu)$. Right: $\kappa(\theta, \mu)$

For small skewness angles $|\theta|$, the jump in the anisotropy ratio κ at the singularity $\mu_0 = \cos 2\theta$ is small. Therefore, for small $|\theta|$, the singularity in the solution is harmless. The fast change in the eigenvector orientation ϕ reflects the fact that for isotropic media ($\kappa = 1$), the orientation of the eigenvectors is arbitrary.

However, for larger skewness angles $|\theta|$, the jump in the anisotropy ratio κ becomes larger, and the error $|\kappa - \mu|$ may be large. This is well demonstrated in Figs. 5 and 6.

The quantity ρ, defined in Eq. (13), is a measure of the change in mean permeability. Solution (24) shows that $\rho = \cos\theta$. Hence, the true mean permeability $(k_1 k_2)^{1/2}$ is always smaller than the apparent mean permeability $(\lambda_1\lambda_2)^{1/2}$. However, for small $|\theta|$, the change is small. For example, for $|\theta| \leq 18°$, the inequality $\cos\theta > 0.95$ is valid.

Inspection of expression (2) shows that the solution $\rho = 1$ may be obtained by a simple change in the two-point flux expression. Replacing Eq. (2) with the flux expression

$$\boldsymbol{f} = \frac{2}{\Delta\xi\,\Delta\eta}\begin{bmatrix}\lambda_1(\Delta\eta)^2\Delta p_\xi \\ \lambda_2(\Delta\xi)^2\Delta p_\eta\end{bmatrix} \tag{32}$$

would yield $\rho = 1$, leaving the expressions for ϕ and κ in solution (24) unchanged. For the resulting $\boldsymbol{K}$, this would give $\lambda_i = \|\boldsymbol{K}\boldsymbol{n}_i\|_2$, $i = 1, 2$. According to the last equation of (8), the vector $\boldsymbol{K}\boldsymbol{n}_i$ is parallel to $\boldsymbol{v}_i$. Hence, Eq. (32) expresses the flux by exploiting that for $\boldsymbol{K}$-orthogonal grids, $(\boldsymbol{K}\boldsymbol{n}_i) \cdot \text{grad}\, p$ is the directional derivative of the pressure along $\boldsymbol{v}_i$, multiplied by $\|\boldsymbol{K}\boldsymbol{n}_i\|_2$.

4 Example 1

Assume a grid skewness angle $\theta = 10°$ and an apparent anisotropy ratio $\mu = 2$. Solution (24) gives the following results, written with two digits,

$$\begin{aligned}\phi &= 8.9°,\\ \kappa &= 2.2,\\ \rho &= 0.98.\end{aligned} \tag{33}$$

Hence, the data given by the user indicate that he is simulating a system where the principal axes are aligned with the grid directions and where the anisotropy ratio is 2. In reality, however, he is simulating a system where the first principal axis is rotated an angle $\phi = 8.9°$ from the first grid direction and where the anisotropy ratio is $\kappa = 2.2$ (see Fig. 7). Also, the mean permeability is 2% smaller than his data indicate.

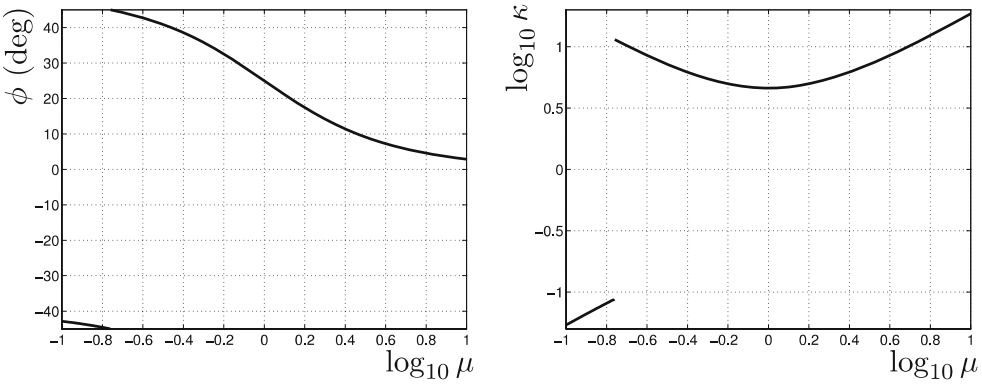

Fig. 6 Solution (24) for $\theta = 40°$. Left: $\phi(\theta, \mu)$. Right: $\kappa(\theta, \mu)$

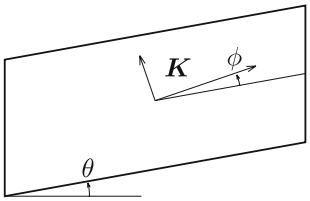

Fig. 7 Illustration of example 1 [Eq. (33)]. Principal directions of the permeability tensor $\boldsymbol{K}$ are denoted by arrows. The anisotropy ratio κ is indicated by the length ratio of the arrows

In the coordinate system of the vector pairs $(\boldsymbol{v}_1, \boldsymbol{n}_2)$ and $(\boldsymbol{n}_1, \boldsymbol{v}_2)$, the permeability tensor [compare Eq. (28)] reads

$$\boldsymbol{K}_{\boldsymbol{v}_1\boldsymbol{n}_2} = (\lambda_1\lambda_2)^{1/2}\begin{bmatrix}1.44 & 0.12\\ 0.12 & 0.69\end{bmatrix},$$
$$\boldsymbol{K}_{\boldsymbol{n}_1\boldsymbol{v}_2} = (\lambda_1\lambda_2)^{1/2}\begin{bmatrix}1.37 & 0.24\\ 0.24 & 0.75\end{bmatrix}. \tag{34}$$

If, for example, $\lambda_1 = 2$ and $\lambda_2 = 1$ in some unit system, then $\boldsymbol{K}_{\boldsymbol{e}_1\boldsymbol{e}_2} = \mathrm{diag}(k_1, k_2) = \mathrm{diag}(2.06, 0.94)$ and

$$\boldsymbol{K}_{\boldsymbol{v}_1\boldsymbol{n}_2} = \begin{bmatrix}2.03 & 0.17\\ 0.17 & 0.97\end{bmatrix}, \qquad \boldsymbol{K}_{\boldsymbol{n}_1\boldsymbol{v}_2} = \begin{bmatrix}1.94 & 0.34\\ 0.34 & 1.06\end{bmatrix}. \tag{35}$$

5 Example 2

The defect of the two-point flux approximation (2) on skew grids is often demonstrated by considering a homogeneous, isotropic medium with three wells, one injector (I) and two producers (P_1 and P_2). The production rate in each of the producers is half the injection rate in the injector. The medium is lying between two impermeable boundaries with the wells located at the boundaries as shown in Fig. 8. The well loci constitute the vertices of an isosceles triangle IP_1P_2, and the angle at each of the vertices P_i, $i = 1, 2$, is 45°. Confer [2] for a similar case.

This system is simulated by discretization of Eq. (1) where the flux is given by Eq. (2) in the control-volume formulation. The grid is a uniform parallelogram grid with skewness angle $\theta = 45°$, as shown schematically in Fig. 9. Homogeneous Neumann conditions are applied at the boundary. To insure that the solution at the flanks is approximately constant, the ratio between the height h and the width b of the gridded domain is chosen equal to 1 : 12. The pressure solution is shown in Fig. 8. The effect of the grid skewness is clearly demonstrated.

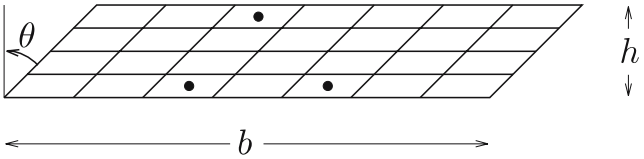

Fig. 9 Skew parallelogram grid with skewness angle $\theta = 45°$ and domain dimensions h and b

Since in this example the skewness angle $\theta = 45°$ and the apparent anisotropy ratio $\mu = 1$, it follows from Eq. (24) that

$$\phi = 22.5°,$$
$$\kappa = 5.8,$$
$$\rho = 0.71. \tag{36}$$

Hence, the simulation on the skew grid is equivalent to solving the three-well system on a medium whose anisotropy ratio is $\kappa = 5.8$ and whose principal direction associated with the largest eigenvalue is rotated an angle $\phi = 22.5°$ from the horizontal axis in the figures (see Fig. 10). A system of point sources and point sinks in a homogeneous medium lying between two infinite, parallel, impermeable boundaries may be solved analytically. The above numerical solution may therefore be compared with the analytical solution of the three-well system, using the permeability tensor given by Eq. (36).

The analytical solution can be determined as follows. Assume first a single point source of strength q in a homogeneous, isotropic medium with permeability k. If the point source lies at the bottom of a semi-infinite strip of width h' (see Fig. 11, left), the solution may be found by applying the conformal mapping

$$w = \sin\frac{\pi z}{h'}. \tag{37}$$

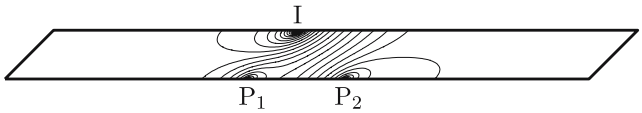

Fig. 8 Pressure contours around the injector I and the producers P_1 and P_2. The angles in the triangle IP_1P_2 at P_i, $i = 1, 2$, are 45°

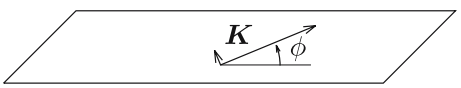

Fig. 10 Permeability tensor $\boldsymbol{K}$ of actually simulated medium. $\phi = 22.5°$

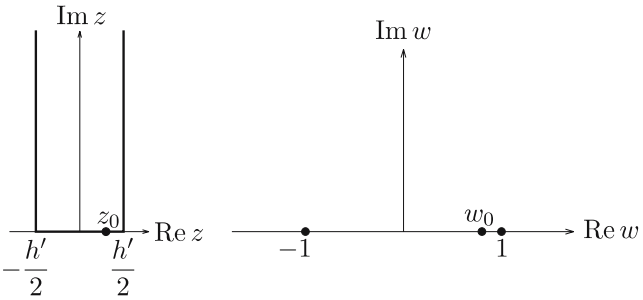

Fig. 11 Transformation from z-plane to w-plane. The well is located at z_0 and w_0, respectively

Transformation (37) maps the semi-infinite strip in the z-plane onto the upper half of the w-plane (see Fig. 11). If the source locus in the w-plane is w_0, the solution is

$$\begin{aligned} p &= -\frac{q}{2\pi k}\ln|w-w_0| \\ &= -\frac{q}{4\pi k}\ln\left[\left(\sin\frac{\pi y'}{h'}\cosh\frac{\pi x'}{h'}-\sin\frac{\pi y'_0}{h'}\right)^2 \right. \\ &\qquad \left. +\left(\cos\frac{\pi y'}{h'}\sinh\frac{\pi x'}{h'}\right)^2\right], \end{aligned} \tag{38}$$

where the primed coordinates $\boldsymbol{x}' = [x',\ y']^{\mathrm{T}} = [\mathrm{Im}\, z,\ -\mathrm{Re}\, z]^{\mathrm{T}}$ are shown in Fig. 12, and where y'_0 is the y'-coordinate of the point source. Since point-source solutions may be superposed, the solution of the three-well problem is obtained by adding solutions (38) for each of the wells.

The solution for an anisotropic medium with permeability tensor $\boldsymbol{K}$ is obtained as follows. The medium is transformed into an isotropic medium with permeability $k = (\det \boldsymbol{K})^{1/2}$ by application of the stretching operator $\boldsymbol{S} = \{s_{i,j}\} = (\det \boldsymbol{K})^{1/4}\boldsymbol{K}^{-1/2}$. Denoting the coordinates of the physical space by $\boldsymbol{x}$ and the coordinates in the stretched space by $\tilde{\boldsymbol{x}}$, the transformation is given by $\tilde{\boldsymbol{x}} = \boldsymbol{S}\boldsymbol{x}$ (see Fig. 13). The horizontal direction in the physical space is then transformed into the vector $\tilde{\boldsymbol{a}} = \boldsymbol{S}[1, 0]^{\mathrm{T}} = [s_{1,1},\ s_{2,1}]^{\mathrm{T}}$.

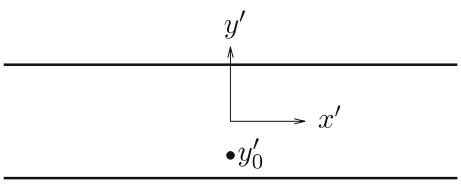

Fig. 12 Coordinate system $\boldsymbol{x}'$. The well is located at $[0,\ y'_0]^{\mathrm{T}}$

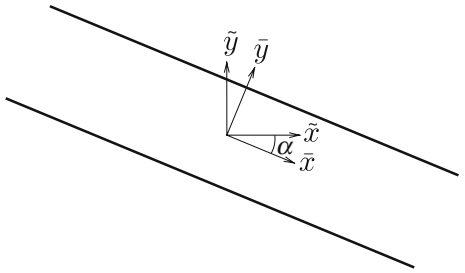

Fig. 13 The rotation $\boldsymbol{R}(\alpha)$ from $\tilde{\boldsymbol{x}} = [\tilde{x},\ \tilde{y}]^{\mathrm{T}}$ to $\bar{\boldsymbol{x}} = [\bar{x},\ \bar{y}]^{\mathrm{T}}$. The shown angle α is negative

Finally, to get from the coordinates $\tilde{\boldsymbol{x}}$ to $\boldsymbol{x}'$, both in the isotropic space, we first apply the rotation $\bar{\boldsymbol{x}} = [\bar{x},\ \bar{y}]^{\mathrm{T}} = \boldsymbol{R}(\alpha)\tilde{\boldsymbol{x}}$ (see Fig. 13) where

$$\alpha = \arctan\frac{\tilde{a}_2}{\tilde{a}_1} = \arctan\frac{s_{2,1}}{s_{1,1}}, \tag{39}$$

and where $\boldsymbol{R}$ is defined in Eq. (27). Then, for each point source, we perform the translation $\boldsymbol{x}' = \bar{\boldsymbol{x}} - [\bar{x}_0,\ 0]^{\mathrm{T}}$, where $\bar{x}_0$ is the $\bar{x}$-coordinate of the point source. Formula (38) applies for the coordinates $\boldsymbol{x}' = [x',\ y']^{\mathrm{T}}$.

Since Neumann conditions apply, both the numerical and the analytical problems are singular. We uniquely define the solution by fixing the pressure at the lower left corner to the same value.

To compare the analytical solution p_a with the numerical solution p_n, we compute the relative error

$$\Delta = \frac{|p_a - p_n|}{\max\{p_n\} - \min\{p_n\}} \tag{40}$$

for all cells, except the well cells where the analytical solution is $\pm\infty$. On a sequence of finer and finer grids, the observed values of $\|\Delta\|_\infty$ decrease monotonically. Due to the singularity at the wells, the decrease is slow. The finest applied grid had 671×61 cells, and on this grid, the maximum relative error was $\|\Delta\|_\infty = 4.5 \times 10^{-3}$.

Note that the results of Eq. (36) show that the preferred flow direction in the grid of Fig. 9 is not along the grid strip combining the injector with the left producer. The preferred flow direction is along the principal axis of the largest eigenvalue. This direction is rotated $\phi = 22.5°$ from the horizontal direction (see Fig. 10). Hence,

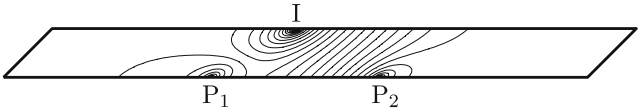

Fig. 14 Pressure contours around the injector I and the producers P_1 and P_2 for the case in which the angles in the triangle $\mathrm{IP}_1\mathrm{P}_2$ at P_i, $i = 1, 2$, are 30°

a larger defect of the two-point flux formula (2) on a grid with skewness angle $\theta = 45°$ may be obtained for a three-well system in which the isosceles triangle IP_1P_2 is not right-angled. The pressure contours for the case in which the angles at P_i, $i = 1, 2$, are 30° are shown in Fig. 14.

6 Conclusions

Simulation with a two-point flux approximation on a skew parallelogram grid corresponds to simulation on a medium whose permeability tensor may be calculated from the user-specified apparent permeabilities. For large skewness, the difference between the found permeability and the apparent permeability may be large. The two-point flux formula may be chosen such that the mean found permeability is equal to the mean apparent permeability.

References

1. Aavatsmark, I.: Introduction to multipoint flux approximations for quadrilateral grids. Comput. Geosci. **6**, 405–432 (2002)
2. Aavatsmark, I., Barkve, T., Bøe, Ø., Mannseth, T.: Discretization on nonorthogonal, quadrilateral grids for inhomogeneous, anisotropic media. J. Comput. Phys. **127**, 2–14 (1996)
3. Aavatsmark, I., Eigestad, G.T., Klausen, R.A.: Numerical convergence of the MPFA O-method for general quadrilateral grids in two and three dimensions: compatible spatial discretizations. In: Arnold, D.N., Bochev, P.B., Lehoucq, R.B., Nicolaides, R.A., Shashkov, M. (eds.) IMA Vol. Ser., **142**, pp. 1–21. Springer, Berlin Heidelberg New York (2006)
4. Eclipse 100 Technical Description. Schlumberger Geoquest (1997)
5. Forsyth, P.A., Sammon, P.H.: Quadratic convergence for cell-centered grids. Appl. Numer. Math. **4**, 377–394 (1988)
6. Klausen, R.A. Winther, R.: Convergence of multipoint flux approximations on quadrilateral grids. Numer. Methods Partial Differ. Equ. **22**, 1438–1454 (2006)
7. Weiser, A. Wheeler, M.F.: On convergence of block-centered finite differences for elliptic problems. SIAM J. Numer. Anal. **25**, 351–375 (1988)